Original Paper

Simulation of degradation phenomena on model enamels with historical compositions[1)]

Carola Troll and Monika Pilz

Fraunhofer-Institut für Silicatforschung (ISC), ISC Branch Bronnbach, Wertheim-Bronnbach (Germany)

Enamels from arts and crafts objects of the Renaissance and Baroque period in Europe show an increasing and irreversible degradation caused by microclimatic environmental influences. In the present study typical degradation phenomena were simulated and the mechanisms of degradation were described. Model enamels on copper substrates were produced and exposed to accelerated weathering in a climate chamber. The enamel compositions were selected according to the analysis of originals. The main part of the work was involved with the investigation of parameters influencing the corrosion of the objects like the effect of pollutants and changes of temperature and humidity. Besides, the influence of mechanical stresses in the enamel layer and the effect of a mechanical pre-damaging were parts of the working programme. The progress of the degradation process was followed by light microscopy and infrared reflectance spectroscopy. The investigations were completed by an assessment of the distribution of the stress in the enamel layer and the metal substrate.

Simulation von Umweltschäden an Modellemails mit historischen Zusammensetzungen

Emails aus kunsthandwerklichen Produktionen der Renaissance und des Barocks in Europa zeigen zunehmend irreversible Schäden, die auf Umwelteinflüsse zurückgeführt werden. In der vorliegenden Studie wurden die typischen Schadensphänomene simuliert und deren Schadensmechanismen beschrieben. Für die Simulation mittels beschleunigter Bewitterung in der Klimakammer wurden Modellemails auf Kupfer hergestellt. Die verwendeten Emailzusammensetzungen wurden hierbei nach Analysenergebnissen von Originalen ausgewählt. Der Kern der Arbeiten war die Untersuchung von verschiedenen Einflußfaktoren wie die Belastung durch Schadgase und Temperatur- und Feuchteschwankungen. Auch der Einfluß mechanischer Spannungen in der Emailschicht und die Wirkung einer vor der Bewitterung in die Emailschicht eingebrachten Vorschädigung waren Teil des Arbeitsprogramms. Der Fortschritt des Verwitterungsprozesses wurde mit Hilfe von Lichtmikroskopie und Infrarot-Reflexions-Spektroskopie verfolgt. Eine Abschätzung der Spannungsverhältnisse in Email und Metall ergänzte die Untersuchungen.

1. Introduction

During the last decades an increasing degradation of enamels from arts and crafts objects of the Renaissance and Baroque period in Europe has been observed. Although these objects are stored indoors, e.g. in museum showcases, they may suffer from an aggressive microclimate. Especially inorganic pollutants like sulphur dioxide and nitrogen dioxide as well as volatile organic compounds like acetic acid and formaldehyde are being considered as a reason for the increasing damage [1 and 2]. These pollutants can be introduced by visitors as well as by air conditioning or they can be emitted by construction materials and even by the objects themselves.

The corrosion of historic enamels on gold, silver or copper substrates leads to a loss of their former glossiness, to a formation of a milky film on the glass surface and to the typical microcracking as known from the glass corrosion processes caused by atmospheric weathering [3 and 4]. In addition, the different thermal expansion coefficients of the enamel layer and the metal substrate cause an increasing growth of cracks within the enamel layer. This finally leads to a flaking off of enamel splinters and consequently to a loss of large enamel surface areas from the objects [1]. Coloured translucent enamels, consisting of alkali alkaline-earth silicate glasses are mostly affected, whereas opaque lead-tin silicate glasses are more stable [5 and 6]. Besides, the substrate itself influences the corrosion progress: The most severe damage can be found on enamelled silver substrates [7 and 8], due to the high thermal expansion coefficient of silver compared to that of glass. The corrosion of the substrate itself as described for copper [9] is also expected to support the flaking off of the enamel.

The characterization of the degradation phenomena and the knowledge of the degradation mechanisms are necessary for the development and the application of effective conservation or restoration measures. Therefore, it was the aim of this study to simulate the degradation phenomenas observed at originals on model enamels and to investigate the fundamental degradation mechanisms.

Received 13 March 1998.

[1)] Presented in German at: 71st Annual Meeting of the German Society of Glass Technology (DGG) on May 27, 1997 in Bayreuth (Germany).

Table 1. Nominal compositions (in wt%) of the enamel types A, B, C and D

enamel type	SiO_2	K_2O	Na_2O	CaO	MgO	Al_2O_3	Fe_2O_3	MnO	CoO	CuO	SO_3	Cl	PbO	SnO
A	54.2	28.2	–	17.0	–	–	–	–	–	–	–	–	–	–
B	59.0	13.4	11.2	6.6	1.6	2.5	0.5	4.1	–	–	–	0.7	–	–
C	68.2	2.7	21.9	0.6	–	0.7	0.7	–	0.7	2.7	0.9	0.8	–	–
D	40.0	5.2	11.6	0.17	1.5	2.0	0.09	0.07	–	0.23	–	–	17.0	21.0

2. Experimental

For the preparation of so-called model enamels three different alkali alkaline-earth silicate glass compositions A, B and C (table 1) were chosen which were expected to show a different chemical resistance. Composition A, a colourless potassium-calcium silicate glass, is identical with the composition of a model glass which has been developed at the Fraunhofer-Institut für Silicatforschung (ISC), Würzburg (Germany), and which is known to be very sensitive to chemical attack [10]. Composition B (a mixed-alkali silicate glass with a reddish colour) and C (a sodium silicate glass with a blue colour) were selected according to the results of chemical elementary analysis of original enamels from the 15th to the 18th centuries [1 and 5]. In addition, an opaque white lead-tin silicate glass was selected (composition D, table 1) because it is described in [5] to be more resistant to atmospheric attack than the alkali alkaline-earth silicate enamels.

Copper was used as metal substrate since this material allows one to study two influences of the substrate on the enamel degradaton: the effect of different thermal expansion coefficients of enamel and metal and the effect of the corrosion of the metal substrate itself. For the preparation of the model enamels copper plates were cut into pieces with a size of $(15 \times 15 \times 1)$ mm^3.

The glasses were melted in a Pt-Rh crucible at temperatures of 1400 to 1500 °C and after 1 h poured onto a brass plate, then crushed and remelted for another hour to improve their homogeneity. The glasses were poured out a second time and ground subsequently. For the reproduction of a constant thickness of the enamel layer the mass of the glass powder needed for a defined thickness was calculated and weighed. The fraction of 20 to 63 µm was applied on the copper plates with a drop of distilled water. After drying in two steps (at 60 and at 200 °C, 5 min each) the samples were heated to temperatures between 830 and 900 °C for 5 min. The characteristic data of the glasses (density, transformation temperature, thermal expansion coefficient and hemispheric temperature) were measured. The data are summarized in table 2 together with the temperature chosen for the enamelling process of each glass composition.

Three different kinds of samples were produced from each composition: enamel layers with two different thicknesses (0.5 and 0.25 mm), both "slowly" cooled down on a ceramic plate to room atmosphere with the natural cooling rate in order to avoid cracks, and one series of specimens "rapidly" cooled down (thickness of enamel layer: 0.5 mm) where cracks were artificially generated by spraying distilled water onto the warm enamel surface. Figure 1 shows some examples of the prepared model enamels.

The degradation phenomena induced by environmental stress were simulated in a climate chamber with a programme with cyclic temperature and relative humidity regulation (programme 1: temperature: $40\,°C > \vartheta > -20\,°C$, relative humidity: $95\,\% > \vartheta > 30\,\%$). The period of one cycle was 12 h and the model enamels were exposed to that programme for up to 7 d. A second weathering programme (programme 2) was chosen to investigate the damaging effect of pollutants: 10 ppm SO_2 were additionally fed into the climate chamber using the same temperature and humidity cycles as described for programme 1. The total weathering time for the specimens was again 7 d.

The corrosion progress of the enamels was followed by nondestructive methods like infrared (IR) reflectance spectroscopy and light microscopy after 4 h (programme 2 only), 1, 3 and 7 d exposure. For the identification of the corrosion products on the enamel surface reference IR spectroscopic measurements were carried out on pure salts. The characterization of the samples was completed by investigations with scanning electron microscopy and energy dispersive element analysis [11].

3. Results and Discussion

3.1 Chemical attack of the atmosphere

The influence of the atmosphere on the degradation of the enamel surfaces will first be described for enamel type C which was remelted according to an original composition and which has a medium chemical resistance to acidic attack compared to the other model enamels.

Figures 2a to c show light microscopic prints of the surfaces of model enamels of type C before weathering and after being exposed to programme 1 (without SO_2) and programme 2 (with SO_2). The exposure time was 7 d for each sample. An increasing formation of crystalline corrosion products after exposure in the SO_2-contaminated atmosphere has been observed.

Table 2. Characteristic data and enamelling temperature of the enamel types A, B, C and D

	enamel A	enamel B	enamel C	enamel D
density in $g \cdot cm^{-3}$	2.6	2.6	2.5	3.3
transformation temperature T_g in °C	610	500	440	–
thermal expansion coefficient $\alpha_{20-300\,°C}$ in $10^{-6}\,K^{-1}$	12.3	11.4	12.2	–
hemispheric temperature in °C	880	810	810	870
firing temperature for the enamelling process in °C	900	830	850	880

Figure 3 represents the IR reflectance spectra of the same type of model enamel recorded after different times of exposure in programme 1. The significant absorption bands at 1065 and 1005 cm^{-1} of the spectra before weathering derive from the Si–O–Si vibration (S-peak) and the Si–O–X vibration (SX-peak, with X = Na, K, Ca). A shift of the SX-peak from 1005 cm^{-1} to lower wave numbers (960 cm^{-1}) is assigned to the leaching of alkali and alkaline-earth ions from the enamel surface. Besides, a shift of the S-peak from 1065 cm^{-1} to higher wave numbers (up to 1075 cm^{-1}) was observed. This proved that there was a generation of ion exchange processes on the enamel surface [3] and the formation of a silica-rich surface layer, the so-called gel layer, due to the attack of the atmosphere. Based on comparative measurements on other enamels (e.g. the more sensitive model enamels of type A) and on selected pure salts, the low intensity absorption band at 1450 cm^{-1} could be identified to derive from a carbonate compound. The leached alkali-ions on the enamel surface had reacted with CO_2 from the atmosphere and had formed crystalline corrosion products.

In contrast, figure 4 shows the IR reflectance spectra of an enamel surface before and after weathering in an SO_2-contaminated atmosphere. After 4 h crystalline corrosion products formed a crust on the enamel surface. The peaks belonging to these corrosion products (1150 and 620 cm^{-1}) are superimposed on the spectrum of the leached enamel surface: they could be identified as sodium sulphate [11]. The changes in the spectra of the leached enamel surface (the shifts of the S-peak from 1065 to 1090 cm^{-1} and the SX-peak from 1005 to 930 cm^{-1}) could be observed only after the removal of the corrosion crust from the enamel surface. The contamination of the atmosphere with SO_2 accelerated the degradation process.

Compared to enamel type C enamels with composition A showed more severe degradation after weathering in the climate chamber. A dense layer of corrosion products on the enamel surface was produced in the "clean" atmosphere (programme 1) after 7 d and in SO_2-contaminated atmosphere (programme 2) only after 4 h. Figure 5 represents the IR reflectance spectra of the enamel surfaces of composition A before and after weathering with both simulation programmes.

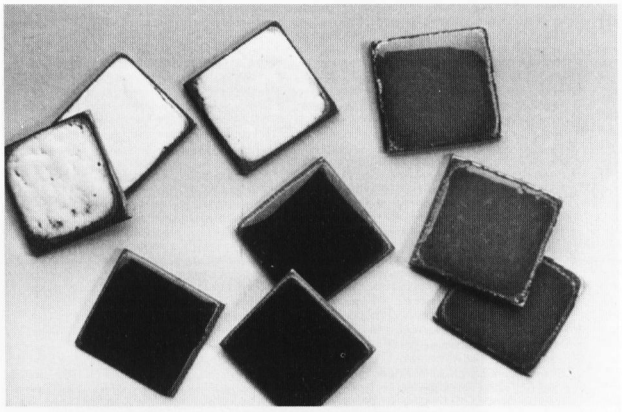

Figure 1. Model enamels.

According to enamel type C the corrosion products on the weathered surface could be identified as carbonates in the case of weathering in an SO_2-free atmosphere and sulphates for weathering in an SO_2-contaminated atmosphere. After an exposure time of 7 d in the climate chamber the corrosion products of some samples were removed and microcracking of the gel layer could be observed. Weathering in the atmosphere with SO_2 (figure 6) produced more and deeper microcracks than weathering in the noncontaminated atmosphere.

Enamel types B and D had a better chemical resistance. Only a few crystals with a size smaller than 5 µm could be detected by light microscopy and no microcracking was found on the enamel surface. The IR reflectance spectra in both cases showed less change than those of enamel composition C.

3.2 Mechanical damage caused by changes in temperature and relative humidity

For the evaluation of the mechanical damage of the enamel layer, it is necessary to distinguish between two kinds of cracks: microcracks which can be observed especially in the gel layer (figure 6) and macrocracks which run across both the gel layer and the glass bulk (figure 7).

The generation of macrocracks, as observed on originals, not only depends on the chemical resistance of the enamels but also on the stress in the composite of

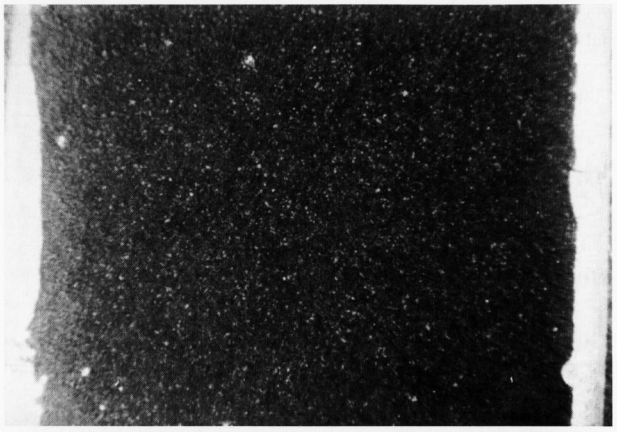

a) ⟷ 1 mm

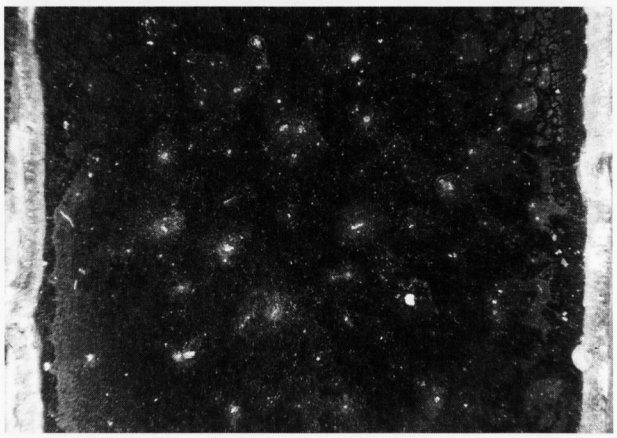

b) ⟷ 1 mm

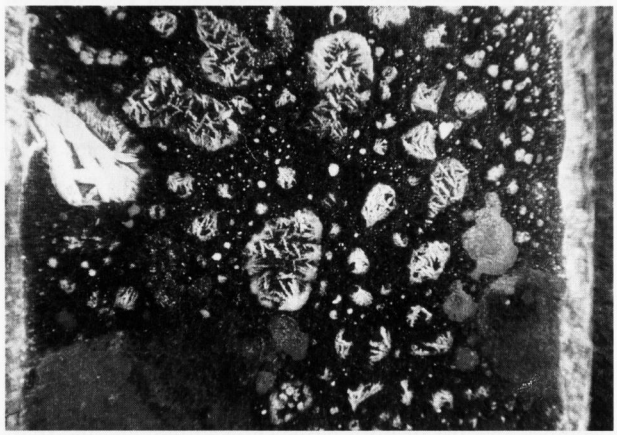

c) ⟷ 1 mm

Figures 2a to c. Light microscopic prints of model enamel of composition C; a) enamel surface before weathering; b) enamel surface after 7 d weathering with programme 1 (without SO_2); c) enamel surface after 7 d weathering with programme 2 (with SO_2).

enamel and metal. Investigations of the conditions under which enamels show macro- as well as microcracking were carried out on model enamels with two different thicknesses of the enamel layer (0.5 and 0.25 mm). The same accelerated weathering conditions as before (programmes 1 and 2) were used.

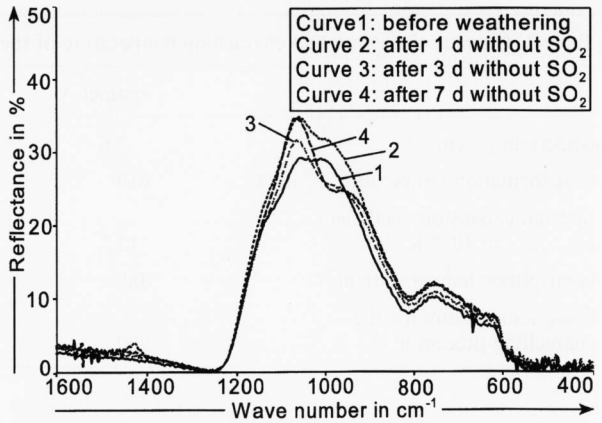

Figure 3. Infrared reflectance spectra of a model enamel of composition C as a function of the weathering time (exposure to programme 1, without SO_2).

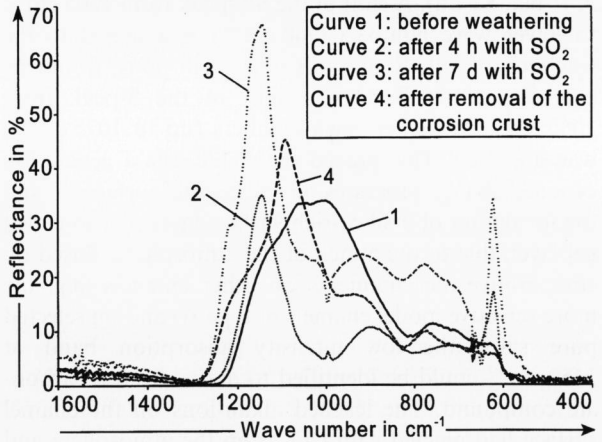

Figure 4. Infrared reflectance spectra of a model enamel of composition C as a function of the weathering time (exposure to programme 2, with SO_2).

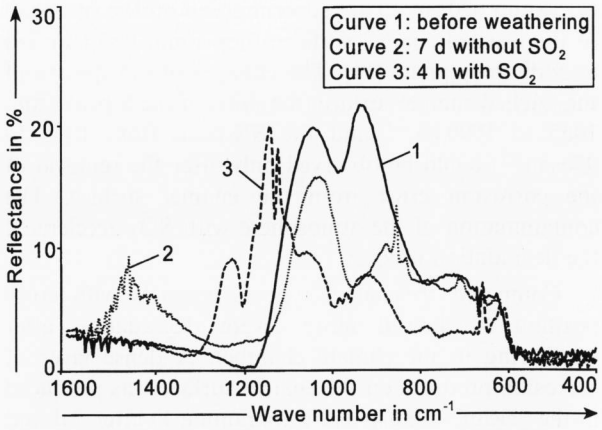

Figure 5. Infrared reflectance spectra of a model enamel of composition A before weathering and after being exposed to programme 1 (without SO_2, 7 d) or programme 2 (with SO_2, 4 h).

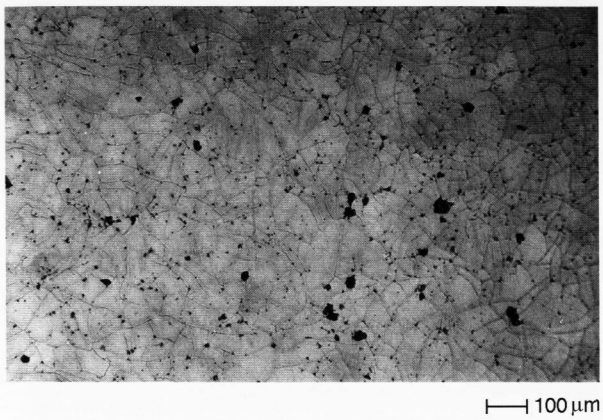

Figure 6. Light microscopic prints of model enamel of composition A, enamel surface after 7 d weathering with programme 2 (with SO_2) and removing of the corrosion crust.

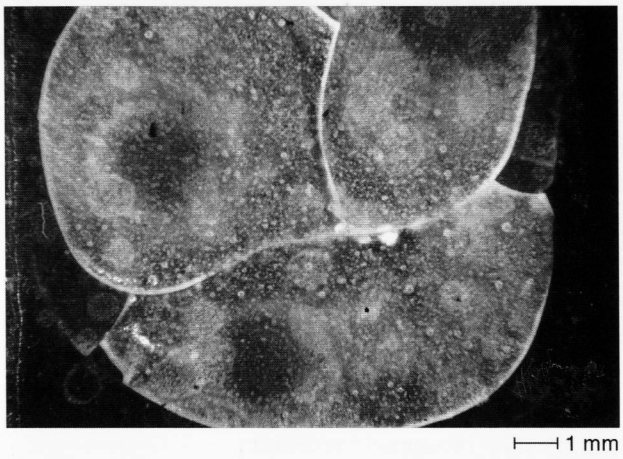

Figure 7. Light microscopic prints of model enamel of composition A, enamel surface after 7 d weathering with programme 1 (without SO_2).

During the exposure time of 7 d microcracks were observed only on model enamels with composition A. The degree of cracking in the gel layer depends on the selected programme and increased with the chemical attack on the enamel surface.

Only one of the thinner (0.25 mm) enamel layers (composition A) showed a narrow macrocrack after 7 d exposure in programme 2. On model enamels of compositions A and B with enamel layers of 0.5 mm thickness, however, heavy macrocrack generation was observed on samples having passed both weathering programmes (figure 7). On model enamels of type C with an enamel layer of 0.5 mm some very narrow long macrocracks were observed after one week of weathering with SO_2-contaminated atmosphere. These tiny cracks were examined only by light microscope and with a 200-fold magnification. The model enamels of type D seemed to be the most stable, because after 7 d weathering even with polluted atmosphere they did not show any cracks.

In order to confirm these observations, the mechanical stresses within the enamel and the metal (copper) were assessed in the following way: For a metal plate which is enamelled only on one side, a bending of the plate due to the compressive strain in the enamel is observed. This results in a distribution of the stress which varies in the cross section of the composite material (figure 8 [12 and 13]). According to [12 and 13] the stress σ_e in the enamel layer and σ_m in the metal substrate can be calculated as a function of the distance x to the enamel/metal interface, if the bending of the substrate is taken into account. The general stress σ can be described by

$$\sigma = \varepsilon \cdot E/(1-\mu) \qquad (1)$$

where $\sigma > 0$ = tensile stress, $\sigma < 0$ = compressive strain, ε = extension, E = modulus of elasticity, and μ = poisson's ratio.

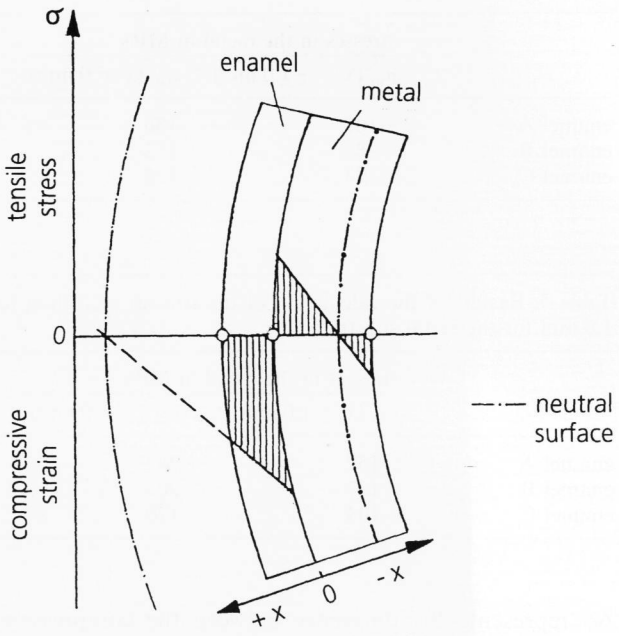

Figure 8. Distribution of the stresses in an enamel/metal composite according to [12 and 13].

The substitution of ε in equation (1) by functions of the moduli of elasticity, the thermal expansion coefficients, the thicknesses and the Poisson's ratios of enamel and metal inclusing the temperature of solidification allows to calculate the stresses σ_e and σ_m [12].

Table 3 summarizes the values needed for the calculations for the enamel compositions A, B and C. For a comparison the stresses σ_e and σ_m at the surface of the enamel and the metal and at the interface enamel/metal were calculated. For enamel composition D not all data could be obtained. The results are presented in table 4 for the enamel thickness of 0.25 mm and in table 5 for the enamel thickness of 0.5 mm.

Table 3. Values for the calculation of the stresses in the enamel/metal composite

	copper	enamel A	enamel B	enamel C
solidification temperature $T_{Sol.}$ (here: T_g in °C [1])	–	610	500	440
thermal expansion coefficient $\alpha_{20\text{-}Tg}$ in 10^{-6} K^{-1} [2]	18.5 (enamel A) 18.1 (enamel B) 17.7 (enamel C)	13.7	13.3	13.1
thickness d in mm	1.0	0.5; 0.25	0.5; 0.25	0.5; 0.25
modulus of elasticity E in GPa [3]	125	61.4	62.6	63.9
Poisson's ratio μ [4]	0.35	0.29	0.23	0.22

[1] enamels: measured
[2] copper: in [14]; enamels: measured
[3] copper: in [15]; enamels: calculated according to Winkelmann and Schott in [16]
[4] copper: in [17]; enamels: calculated according to Winkelmann and Schott in [16]

Table 4. Results of the calculation of the stresses according to [11 and 12] for a thickness of 0.25 mm for the enamel layer and of 1.0 mm for the metal substrate

	stresses in the metal in MPa		$\Delta\sigma$ at the interface in MPa	stresses in the enamel in MPa	
	σ_m (x = −1.0 mm)	σ_m (x = 0 mm)		σ_e (x = 0 mm)	σ_e (x = 0.25 mm)
enamel A	−107	186	344	−158	−127
enamel B	−88	152	275	−123	−97
enamel C	−73	126	228	−102	−81

Table 5. Results of the calculation of the stresses according to [11 and 12] for a thickness of 0.5 mm for the enamel layer and of 1.0 mm for the metal substrate

	stresses in the metal in MPa		$\Delta\sigma$ at the interface in MPa	stresses in the enamel in MPa	
	σ_m (x = 1.0 mm)	σ_m (x = 0 mm)		σ_e (x = 0 mm)	σ_e (x = 0.5 mm)
enamel A	−152	247	378	−131	−42
enamel B	−127	205	305	−100	−30
enamel C	−104	170	253	−83	−25

$\Delta\sigma$ represents the difference between the compressive strain in the enamel and the tensile stress in the metal at the interface enamel/metal (x = 0 mm).

It is known that the possibility of a macrocrack generation in the enamel layer increases with a decreasing compressive strain in the enamel surface and an increasing stress difference $\Delta\sigma$ at the enamel/metal interface. A comparison of the values in tables 4 and 5 shows that the sensitivity for crack generation in dependance of the enamel compositions decreases in the following way: A > B > C. As expected, thinner enamel layers should be more stable against mechanical stresses than thicker layers.

In addition to the stress within the object itself, the variations of stress due to the temperature changes during the weathering cycle were assessed according to equation (2)

$$\sigma = \Delta T \cdot \Delta\alpha \cdot E \,. \qquad (2)$$

For temperature changes of ΔT = 60 K (both programmes: −20 to 40 °C) an average of $\sigma \approx$ 17 MPa could be obtained. The assessed values of stresses induced by accelerated weathering (ca. 17 MPa) and the assessed values of stresses of the compressive strain in the enamel surface (25 to 42 MPa) are of the same order of magnitude. If the compressive strain in the enamel surface could be overcompensated by the induced stress, the generated tensile stress will lead to a crack growth. Therefore, it can be concluded that the macrocracks in the thicker enamel layers were caused by the change in temperature.

3.3 Effect of mechanical pre-damage

Macrocracks that have been caused, e.g., by former rough handling of the object, can also affect the degradation process. In a humid atmosphere a thin film of water molecules covers the enamel surface. The thickness of this film depends on the relative humidity and

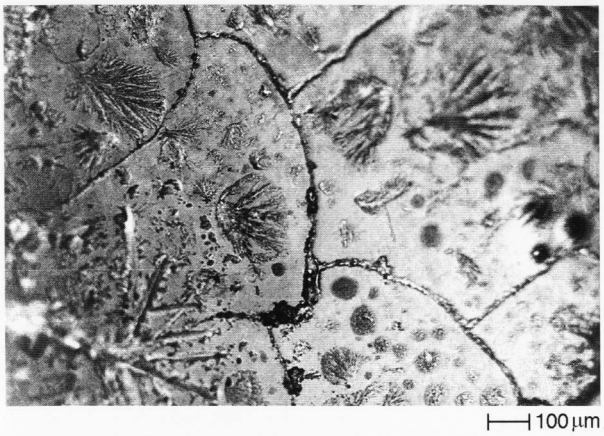

Figure 9. Light microscopic prints of model enamel of composition C, crystal growth in macrocracks on a pre-damaged enamel after 1 d exposure to programme 2 (with SO_2).

changes in the relative humidity cause drying and humidifying of the enamel surface. During the drying of the surface, capillary forces retain the water at the end of the cracks and the surface in the crack is drying more slowly. The corrosion process therefore will be accelerated in these cracks compared to the corrosion rate beneath the cracks.

Besides, the growth of crystals in the macrocracks can induce mechanical stress in the enamel layer. This leads to the growth of cracks and finally to a flaking off of enamel splinters. As an example figure 9 shows a pre-damaged model enamel of type C and the growth of crystals in the cracks after 1 d exposure in the climate chamber with SO_2. Especially for the model enamels of type A and C with a lower chemical resistance the flaking off initiated by crystal growth was observed.

The degree of damage depends on the induced stresses and therefore on the extent of pre-damage as well as on the type of crystals. Some kinds of crystals e.g. sodium carbonate or sodium sulphate have a high expansion depending on the degree of hydration. Their expansion of volume can reach up to 400 %. These salts have the same destructive effect in the cracks of the enamels as already known for the pores of natural stone.

3.4 Effect of the substrate

The metal substrate influences the enamel degradation mainly in two ways. The first, described in the literature [1, 7 and 8], depends on the difference of thermal expansion of metal and enamel. Especially the high thermal expansion coefficient of silver ($\alpha_{0-300\,°C} = 20.3 \cdot 10^{-6}\,K^{-1}$ [13]) compared to gold ($\alpha_{0-300\,°C} = 14.8 \cdot 10^{-6}\,K^{-1}$ [13]) and copper ($\alpha_{0-300\,°C} = 17.2 \cdot 10^{-6}\,K^{-1}$ [13]) leads to a higher loss of the enamel layer which can reach up to 70 % of the enamelled silver surface [7].

The second effect depends on the corrosion of the metal substrate itself. Especially copper shows heavy corrosion phenomena under acidic conditions like in weathering programme 2 (with SO_2). Copper salts which migrate from the corroding copper substrate into the cracks of the enamel layer can cause stress in the enamel layer. This too can lead to the growth of the cracks and finally to the flaking off of enamel splinters. Besides, contaminated water can penetrate into deep cracks and cause the corrosion of the copper substrate under the enamel layer. Especially on the colourless enamel type A which is very sensitive to chemical and mechanical attack the green copper sulphates from the corrosion progress could be identified at the edges of the model enamels and in deep cracks in the enamel layer.

4. Conclusion

The typical degradation phenomena like loss of glossiness, cracking and flaking off of the enamel layer have been successfully reproduced on model enamels by accelerated weathering in a climate chamber. It was found that the enamel degradation is a complex interaction between different chemical and mechanical effects.

Ion exchange processes accelerated by acidic pollutants such as SO_2 weaken the glass surface, a gel layer with a lower mechanical resistance compared to the bulk glass is formed. Additionally the enamels suffer from mechanical stresses due to the different thermal expansion coefficients of enamel and metal. These basic stresses in the model samples themselves were assessed by a calculation according to [12 and 13] to estimate the stability of different enamel compositions. The calculations could be qualitatively confirmed by experimental data which show that one of the main degradation factors is the mechanical stress in the enamel layer. The stress is influenced by factors like changes of temperature or the chemical degradation of the objects. Corrosion products deriving from the enamel layer or metal substrate can grow in cracks and widen them. Even changes in the relative humidity can have an additional destructive effect. If the humidity is decreasing, the gel layer is drying and forming microcracks. These microcracks can be starting points for subsequent macrocracks.

With these simulation experiments the dependance of the degradation process of enamels on environmental parameters could be studied. First recommendations on storage conditions for endangered objects were derived. Further experiments will include investigations on the corrosive effects of formaldehyde and acetic acid.

5. References

[1] Müller, W. (ed.): Modellhafte Untersuchungen zu Umweltschädigungen in Innenräumen anhand des Grünen Gewölbes. BAM-Forschungsbericht 215. Bremerhaven: Wirtschaftsverl. NW, 1995.

[2] Pilz, M.; Troll, C.: Simulation of gold enamel degradation. In: Bradley, S. (ed.): The interface between science and conservation. Brit. Museum Occ. Papers no. 116. London: British Museum Press, 1997. p. 193–201.

[3] Clark, D. E.; Zoitos, B. K. (eds.): Corrosion of glass, ceramics and ceramic superconductors. New Jersey: Noyes Publ., 1992.
[4] Müller, W.; Torge, M.; Adam K.: Primary stabilization factor of the corrosion of historical glasses: the gel layer. Glastech. Ber. Glass Sci. Technol. **68** (1995) no. 9, p. 285–292.
[5] Eveno, M.; Fromageot, D.; Kusko, B. et al.: Etude de l'altération d'une plaque émaillée attribuée à la production de Limoges. In: ICOM Committee for Conservation – 9th Triennial Meeting, Dresden 1990. Preprints Vol. I. London: James & James, 1990. p. 18–23.
[6] Smith, R.; Carlson, J. H.; Newman, R. M.: An investigation into the deterioration of painted limoges enamel plaques c. 1470–1530. Stud. in Conserv. **32** (1987) p. 102–113.
[7] Zamora Campos, B.; Schmitz, I.; Clark, A. et al.: Transluzides burgundisches Email auf Silber. Pt. 1. Restauro **101** (1995) no. 5, p. 322–325.
[8] Zamora Campos, B.; Schmitz, I.; Clark, A. et al.: Transluzides burgundisches Email auf Silber. Pt. 2. Restauro **101** (1995) no. 6, p. 418–421.
[9] Perez y Jorba, M.; Rommeluere, M.; Mazerolles, L.: Etude de la détérioration d'une plaque d'émail peint de Limoges. Stud. in Conserv. **38** (1993) p. 206–212.
[10] Fuchs, D. R.; Römich, H.; Schmidt, H.: Glass sensors: assessment of complex corrosive stresses in conservation research. In: Vandiver, P. B.; Druzik, J.; Wheeler, G. S. (eds.): Materials issues in art and archaeology II. Symp. San Francisco, CA, 1990. Mat. Res. Soc. Symp. Proc. **185** (1991) p. 239–251.
[11] Troll, C.: Untersuchungen zu Schadensphänomenen an Emails und Glasuren. Julius-Maximilians-Universität Würzburg, Diss. 1998.
[12] Oel, H. J.: Berechnung der inneren Spannungen von Schichtwerkstoffen. VDI Z **108** (1966) p. 1727–1729.
[13] Dietzel, A. H.: Emaillierung – Wissenschaftliche Grundlagen und Grundzüge der Technologie. Berlin (et al.): Springer, 1981. p. 133–139.
[14] Beitz, W.; Küttner, K.-H. (eds.): Dubbel, Taschenbuch für den Maschinenbau. 18th ed., Berlin (et al.): Springer, 1995. p. D 42.
[15] Petzold, A.; Pöschmann, H.: Email und Emailliertechnik. Leipzig: Deutscher Verl. Grundstoffind., 1992. p. 156.
[16] Scholze, H.: Glas – Natur, Struktur und Eigenschaften. 3rd rev. ed., Berlin (et al.): Springer, 1988. p. 233–234.
[17] Ardenne, M. v.: Tabellen zur angewandten Physik. 3rd vol. Berlin: VEB Deutscher Verl. der Wissenschaften, 1973. p. 6.

1098P003

Address of the authors:

C. Troll, M. Pilz
Fraunhofer-Institut für Silicatforschung (ISC), Würzburg
Außenstelle Bronnbach
Bronnbach 28
D-97877 Wertheim-Bronnbach